

Decoupling Bidirectional Geometric Representations of 4D cost volume with 2D convolution

Xiaobao Wei^{1,2} Changyong Shu^{1*} Zhaokun Yue¹ Chang Huang²
 Weiwei Liu² Shuai Yang² Lirong Yang² Peng Gao²
 Wenbin Zhang² Gaochao Zhu² Chengxiang Wang²

¹ Nanjing University of Science and Technology ² Carizon
 wxb@njust.edu.cn

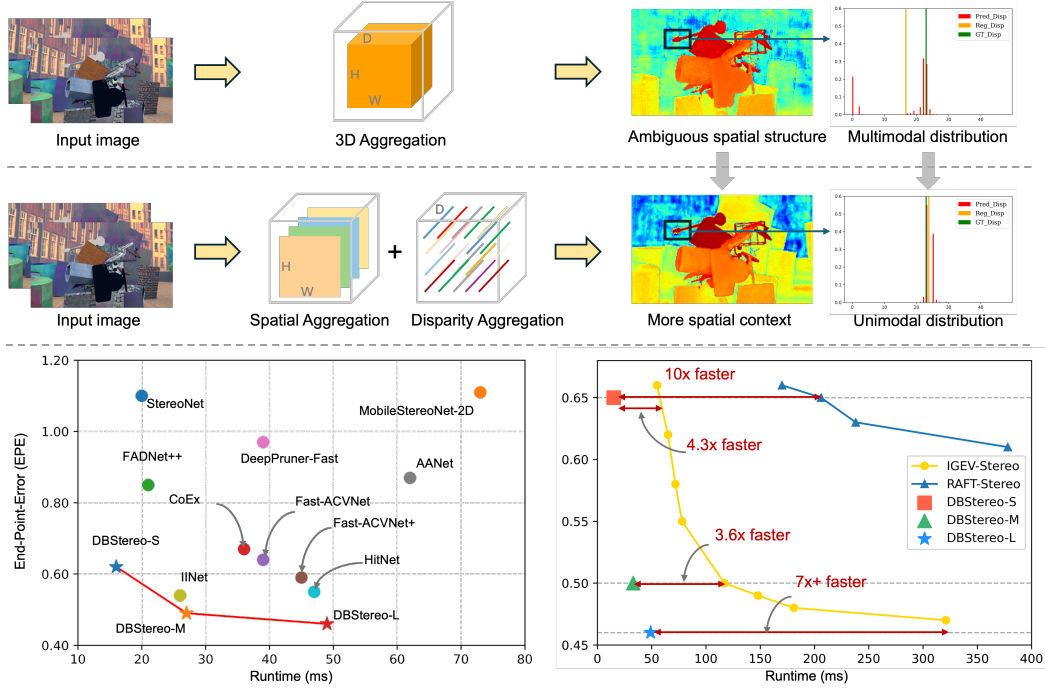


Figure 1: The proposed DBStereo decouple the traditional 3D aggregation into spatial aggregation and disparity aggregation which is based on 2D convolutions. The spatial aggregation can incorporate more spatial structure context and the disparity aggregation make the prediction of disparity more concentrated around the ground truth. Our DBStereo outperforms all existing aggregation-based methods [1, 5, 12, 13, 21, 22, 23, 28, 32, 33] in both inference time and accuracy, even surpassing the iterative-based method (RAFT-Stereo [15] and IGEV-Stereo [30]).

Abstract

High-performance real-time stereo matching methods invariably rely on 3D regularization of the cost volume, which is unfriendly to mobile devices. And 2D regularization based methods struggle in ill-posed regions. In this paper, we present a deployment-friendly 4D cost aggregation network DBStereo, which is based on pure 2D convolutions. Specifically, we first provide a thorough analysis of the decoupling characteristics of 4D cost volume. And design a lightweight bidirec-

tional geometry aggregation block to capture spatial and disparity representation respectively. Through decoupled learning, our approach achieves real-time performance and impressive accuracy simultaneously. Extensive experiments demonstrate that our proposed DBStereo outperforms all existing aggregation-based methods in both inference time and accuracy, even surpassing the iterative-based method IGEV-Stereo. Our study break the empirical design of using 3D convolutions for 4D cost volume and provides a simple yet strong baseline of the proposed decouple aggregation paradigm for further study. Code will be available at (<https://github.com/happydummy/DBStereo>) soon.

1 Introduction

Stereo matching has remained a core challenge in computer vision over the past decade, continuously advancing critical applications such as autonomous driving[35], industrial robotics[10], and augmented reality[36]. The essence of the technology lies in establishing accurate pixel-level correspondences between left and right images. However, under the resource-constrained conditions of edge computing devices, simultaneously achieving high matching accuracy and real-time inference remains a significant bottleneck.

With the evolution of deep learning, end-to-end stereo matching frameworks have gradually become mainstream. One of the representative works is PSMNet [2], which constructs a 4D cost volume and utilizes 3D convolutional network to aggregate it. Such 4D cost aggregation paradigm methods [3, 6, 14, 19, 27] achieve significant breakthroughs on GPU devices. However, the redundant information inherent in 4D cost volumes force the model to rely on computationally expensive 3D convolutions for regularization, posing substantial difficulties for mobile deployment. In recent years, iterative optimization paradigms [16, 24, 31, 25], have demonstrated superior performance. Unlike previous aggregation-based methods, these approaches construct 3D correlation cost volumes and progressively refine disparity maps through iterative indexing it, thereby avoiding complex cost aggregation. While reducing computational complexity, the lack of cost aggregation results in cost volumes deficient in global geometric information, leading to disparity discontinuities in occluded regions, mismatches in textureless areas, and artifacts on reflective surfaces. More critically, achieving acceptable accuracy often requires multiple iterations, resulting in inference delays exceeding 100 ms for most methods, which hinders their applicability in real-time scenarios.

Real-time stereo matching research [1, 5, 12, 13, 21, 22] can be categorized into two types: 2D CNNs based and 3D CNNs based. Both of them made significant compromises: AANet [34] constructs a 3D correlation cost volume and enhances performance in pathological regions by using deformable convolutions, but its specialized operators pose challenges for deployment on edge devices; MobileStereoNet-2D [21] attempts a pure 2D convolutional architecture but suffers severe performance degradation; DeepPruner [7] narrows the search space by pruning the 4D cost volumes, ACVNet [28] filters redundant information via attention weights, yet both still rely on 3D CNNs for aggregation. Empirically, it appears that the informative 4D cost volume can not escape its dependence on 3D CNNs.

In fact, these methods overlook inherent limitations of 3D CNNs in stereo matching: spatial and disparity dimensions share the same receptive fields, while disparity aggregation requires a global receptive field, which leading to degradation; the coupled learning of spatial and disparity features increases model training difficulty. Although FoundationStereo [26] recognizes the need for different receptive fields of two dimensions and decomposes a 3D convolution into a spatial 3D convolution and a disparity 3D convolution, it remains a localized refinement of standard 3D convolution rather than addressing the fundamental issue of coupled learning.

In this paper, we propose a novel pure 2D CNN-based framework for 4D cost aggregation that simultaneously achieves real-time performance and high accuracy. We first provide an in-depth analysis of the limitations of 3D regularization networks and introduce our spatial-disparity decoupled aggregation paradigm. Specifically, we first use Channel2Disp operator to transform the 4D cost volume to the 3D one. Then, through our designed Bidirectional Geometry Aggregation (BGA) block consisting of Spatial Aggregation module and Disparity Aggregation module, we decouple the geometric representation of the cost volume into spatial and disparity dimensions. By leveraging 2D CNN-based bidirectional geometric representation decoupling, our method achieves significant

improvement. More importantly, our work pioneers a new technical pathway for high-accuracy real-time stereo matching.

Our main contributions are as follows:

- We provide a thorough analysis of the geometric representation of 4D cost volume, breaking away from the traditional coupled aggregation paradigm based on 3D convolutions, and establish a simple yet strong baseline for efficient 4D cost aggregation.
- We design a pure 2D convolutional Bidirectional Geometry Aggregation block to independently capture spatial and disparity representation of the 4D cost volume.
- We demonstrate the effectiveness of our approach, achieving state-of-the-art performance on multiple benchmarks. The proposed decouple aggregation paradigm opens up a new research direction for the community.

2 Related work

Cost aggregation paradigm stereo matching methods [7, 9, 11, 28, 34] typically follow a four-stage pipeline: feature extraction, cost volume construction, cost aggregation, and disparity regression. Among these, the cost volume serves as the core basis for matching decisions, and its construction quality directly affects final performance.

Cost volume construction: Existing cost volume representation can be divided into two categories: the concatenation volume and the correlation volume. GC-Net [11] directly concatenate the features maps of left and right images to construct a 4D concatenation cost volume for all disparities. This dense 4D concatenation volume retains comprehensive information from all channels, and thus exhibit enhanced performance. However, excessive redundant information forces the model to rely on a large amount of 3D convolutions to aggregate and regularize the 4D cost volume, which means high computational and memory cost. RAFT-Stereo [15] employs the all-pairs correlation constructed based on a similarity matrix derived from left and right image features. However just calculates the feature correlation matrix lacks non-local information and struggling in ill-posed regions. GwcNet [9] designed a group-wise correlation cost volume that combines the advantage of these two cost volumes. IGEV-Stereo [30] constructs a geometry encoding volume incorporating context information and local matching clues.

Cost aggregation: In order to filter the redundant noise on cost volume, cost aggregation consumes a significant amount of computational resources. DiffuVolume [37] design an effective diffusion-based framework which casts the information filtering as the denoising process of the diffusion model. ACVNet [28] proposed the attention mechanism to filter the cost volume and significantly alleviated the burden of cost aggregation. BANet [29] utilized spatial attention to separate high-frequency edge regions and low-frequency smooth regions of cost volume. However, these methods still require stacked 3D convolutions to regularize the 4D cost volumes. **Empirically, it seems that high-dimensional cost volume inevitably require dimension-matched convolution to capture the internal correspondences.**

3 Is 3D Convolution Necessary for 4D Cost Aggregation?

In learning-based stereo matching, constructing a 4D cost volume (of dimensions $(D \times C \times W \times H)$) and applying regularization form the foundation of state-of-the-art paradigms [2, 9, 11, 28]. A widely adopted convention is to directly employ 3D CNNs to process this 4D tensor. The underlying intuition is powerful and seemingly natural: a high-dimensional tensor appears to inherently require convolution operations of matching dimensionality to capture the complex, intertwined relationships across all its dimensions.

However, this empirical design prompts a critical reflection: Is this dimension-matched design truly necessary or optimal? Could it potentially introduce redundancy or even noise? This section delves into the inherent limitations of 3D regularization networks for stereo matching, thereby motivating our novel spatial-disparity decoupled aggregation paradigm based on pure 2D convolutions.

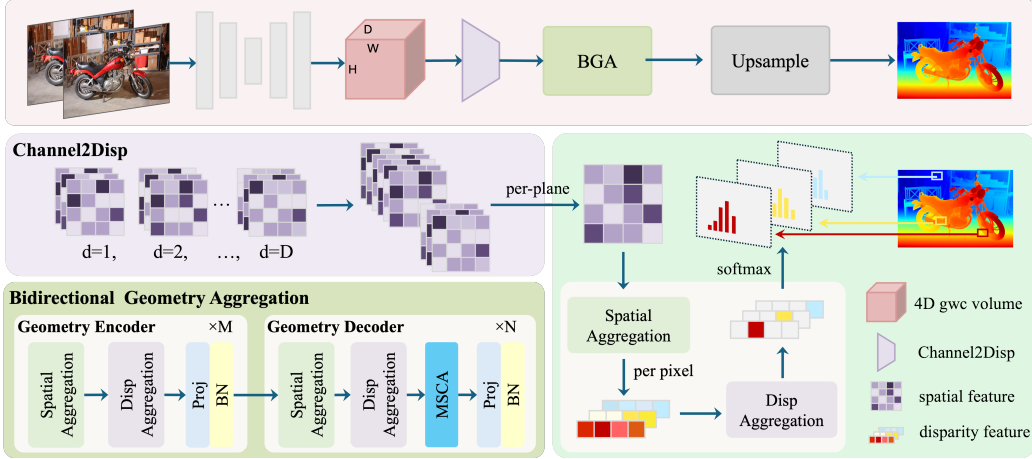


Figure 2: The framework of our proposed DBStereo. The Bidirectional Geometry Aggregation (BGA) block is stacked with multiple Spatial Aggregation modules and Disparity Aggregation modules. The Spatial Aggregation module extracts spatial context for each plane of the cost volume and the Disparity Aggregation modules performs global receptive field filtering on each pixel.

3.1 Limitations of Traditional 3D Regularization Network

In stereo matching based on 4D cost volumes, traditional aggregation paradigms commonly employ 3D convolutions for cost aggregation. Yet, this paradigm suffers from two inherent flaws:

Coupled Aggregation Pattern: The traditional paradigm enforces the use of 3D convolution kernels (e.g., $3 \times 3 \times 3$) to extract features from both spatial and disparity dimensions simultaneously. It implicitly assumes that spatial context and disparity context exhibit consistent aggregation patterns within local regions. However, this assumption is not hold true and could instead constrain the model’s expressive capability, making it more susceptible to overfitting noise and non-essential patterns in the training data.

Slow Receptive Field Expansion in Disparity Dimension: Due to the coupled aggregation pattern, the expansion of the receptive field in the disparity dimension is inherently tied to that in the spatial dimensions. Constrained by the kernel size, each 3D convolution operation can only increase the receptive field in the disparity direction marginally (e.g., a $3 \times 3 \times 3$ kernel increases it by only 2). To capture sufficient disparity context, a deep stack of 3D CNNs layers is required, directly leading to a dramatic increase in computational cost and memory consumption.

3.2 Spatial-Disparity Decoupled Aggregation Paradigm

Based on the above shortcomings, we conducted a thorough analysis of the inherent properties of stereo matching tasks and summarized the following task-specific priors.

Spatial Local Smoothness Prior: Adjacent pixels at the same depth possess similar disparity values. This prior is particularly beneficial in low-frequency, textureless regions.

Disparity Unimodality Prior: For a single pixel, the correct disparity value should be unique, meaning the disparity probability distribution should be a sharp unimodal distribution.

We propose a novel spatial-disparity decoupled aggregation paradigm that explicitly encodes these two inherent prior into our network architecture, thereby introducing a powerful inductive bias. Specifically, we reshape the high-dimensional 4D cost volume ($D \times C \times W \times H$) into a 3D tensor ($D \cdot C \times W \times H$), decoupling the traditional 4D cost aggregation into two successive pure 2D convolution steps:

Spatial Aggregation: A 2D convolution (e.g., with a 3×3 kernel) is applied to the spatial dimension of reshaped cost volume ($D \cdot C \times W \times H$). This step focuses on aggregating spatial context within

the same disparity level, effectively smoothing image noise and resolving matching ambiguities in areas like textureless regions.

Disparity Aggregation: Traditional 3D CNNs with their limited local receptive field in disparity dimension struggle to capture long-range dependencies, often resulting in a blurred/tailed distribution or a multi-modal distribution at edges or a flat distribution in textureless areas. We aim for each aggregation along the disparity dimension to possess a global receptive field and apply 2D CNNs with a 1×1 kernel to the features after spatial aggregation. It is noteworthy that this 1×1 convolution essentially performs a global, fully-connected-style interaction across the entire disparity dimension (D), achieving highly efficient optimization of the disparity context. Through this design, our disparity aggregation module enables comparison and competition across the global disparity range, effectively suppressing incorrect disparity responses and facilitating the formation of a more reasonable, sharper unimodal probability distribution, leading to clearer object boundaries.

3.3 Conclusion

In summary, compared to coupled 3D CNNs, our decoupled structure imposes highly precise inductive biases: spatial aggregation enforces *spatial local smoothness prior*, while disparity aggregation enforces *disparity unimodality prior*. By incorporating these inductive biases into the network architecture, we have significantly reduced the model’s search space. The model no longer needs to implicitly learn these fundamental rules from vast amounts of data but instead learns higher level feature representations directly under these inductive biases. This significantly mitigates the risk of the model overfitting to noisy data, thereby achieving a regularization effect far surpassing that of traditional 3D CNNs.

4 Methods

In this section, we introduce the detailed structure of our proposed DBStereo. As shown in Fig 2, unlike previous approaches utilizing 3D CNNs, we decouple the 3D regularization network into a bidirectional geometry aggregation module based on purely 2D CNNs: disparity aggregation module and spatial aggregation module.

4.1 Feature Extractor

We employ MobileNetV2 ([20]) pretrained on ImageNet ([4]) as our backbone to extract multi-scale feature maps $\{\mathbf{f}_{l,i}, \mathbf{f}_{r,i} \in \mathbb{R}^{C_i \times \frac{H}{i} \times \frac{W}{i}}\}, i = 4, 8, 16, 32$. And a cascade of upsampling blocks are utilized to restore the feature maps to 1/4 resolution of input image. Finally, we obtain multi-scale feature maps $F_{l,i}, F_{r,i} \in \mathbb{R}^{C_i \times \frac{H}{i} \times \frac{W}{i}}, i = 4, 8, 16$. Among them, $F_{l,4}, F_{r,4}$ are used to construct the 4D cost volume for subsequent disparity prediction, while $F_{l,4}, F_{l,8}, F_{l,16}$ are utilized to generate spatial attention, further enhancing the robustness of disparity estimation.

4.2 Cost volume construction

We construct a 4D group-wise correlation volume [9] with features extracted from the left and right images. The left and right features are split into groups and computing correlation maps group by group.

$$\mathbf{C}_{gwc}(d, x, y, g) = \frac{1}{N_c/N_g} \langle \mathbf{f}_l^g(x, y), \mathbf{f}_r^g(x - d, y) \rangle, \quad (1)$$

where N_c denotes the number of feature channels, N_g denotes the number of groups and d denotes the all disparity candidates.

4.3 Cost aggregation

Given the 4D group-wise cost volume, we first use the Channel2Disp operator to fuse the feature dimension and the disparity dimension of the original cost volume. The core idea of our Channel2Disp

transformation is to concatenate the feature maps from all disparity levels, converting the 4D geometric representation into a dense 3D representation without altering spatial structure. Specifically, we reshape the volume as follows:

$$C_{3D} = \text{Reshape}(C_{gwc}) \in \mathbb{R}^{(G \cdot D) \times H \times W} \quad (2)$$

This operation explicitly encodes the disparity context into a unified dimension and allows our network to leverage the power of standard 2D convolutions to reason about complex 4D geometric representations without the overhead of 3D operations.

The reconstructed 3D cost volume C_{3D} is coupled complex spatial information and disparity information. To efficiently extract required geometric representation, we propose the Bidirectional Geometry Aggregation (BGA) block with encoder-decoder architecture. The proposal of the BGA is based on the theoretical analysis in Section 3. We construct the BGA by repeatedly stacking spatial aggregation modules and disparity aggregation modules.

4.4 Disparity Prediction

After obtaining the aggregated cost volume, we apply the softmax operation to it to regress the disparity map d_0 :

$$\mathbf{d}_0 = \sum_{d=0}^{D_{max}/4-1} d \times \text{Softmax}(\mathbf{C}_{agg}(d)), \quad (3)$$

where D_{max} denotes the predefined maximum disparity. The disparity map d_0 is at 1/4 resolution of input images. We utilize interpolation and learnable parameters respectively to upsample the disparity map d_0 to full resolution for supervision.

4.5 Loss Function

We employ the smooth L_1 loss to supervise our network. The loss is defined as follow:

$$\mathcal{L} = \lambda_0 \text{Smooth}_{L_1}(\mathbf{d}_{init} - \mathbf{d}_{gt}) + \lambda_1 \text{Smooth}_{L_1}(\mathbf{d}_{final} - \mathbf{d}_{gt}) \quad (4)$$

where d_{gt} is the ground truth of disparity and $\lambda_0 = 0.3, \lambda_1 = 1$.

5 Experiments

5.1 Datasets and Evaluation Metrics

Scene Flow [17] is a large-scale synthetic stereo dataset containing 35,454 training and 4,370 testing stereo image pairs at 960x540 resolution. This dataset provides dense disparity maps as ground truth. In evaluations, we utilize the end point error (EPE) and the D1 outlier as the evaluation metrics, where EPE is the average l_1 distance between the prediction and ground truth disparity. And D1 denotes the percentage of outliers with an absolute error greater than 1 pixels.

KITTI is a real-world dataset consisting of KITTI 2012 [8] and KITTI 2015 [18]. KITTI 2012 provides 194 training pairs and 195 testing pairs, and KITTI 2015 provides 200 training pairs and 200 testing pairs. Both datasets provide sparse ground-truth disparities obtained with LiDAR. For evaluations, we calculate EPE and the percentage of pixels with EPE larger than 3 pixels in all (D1-all) regions. All two KITTI datasets are also used for cross-domain generalization performance evaluation, with EPE and >3px metric (i.e., the percentage of points with absolute error larger than 3 pixels) reported.

5.2 Implementation Details

We have implemented our methods using PyTorch and conducted experiments on 8 NVIDIA RTX 3090 GPUs. We train our pretrained model on Scene Flow dataset for 90 epochs. For the KITTI dataset evaluation, we fine-tune the pre-trained model for 500 epochs using a mixed training set comprising KITTI 2012 and KITTI2015 training datasets.

Table 1: Comparison with the state-of-the-art methods on SceneFlow. Runtime is measured on an RTX 3090 GPU.

Paradigm	Method	EPE (px)	D1 (%)	Runtime (ms)
Cost aggregation	PSMNet [2]	1.09	12.1	317
	StereoNet [12]	1.10	-	20
	AANet [34]	0.87	9.3	93
	AANet+ [34]	0.72	7.4	87
	MobileStereoNet-2D [21]	1.11	-	73
	FADNet++ [23]	0.85	-	21
	CoEx [1]	0.67	4.02	36
	Fast-ACVNet [32]	0.64	2.31	39
	Fast-ACVNet+ [32]	0.59	2.08	45
	IINet [13]	0.54	2.18	26
	BANET-2D [29]	0.57	2.50	xx
	BANET-3D [29]	0.51	2.21	xx
Iterative optimization	RAFT-Stereo [15]	0.61	2.85	380
	IGEV-Stereo [30]	<u>0.47</u>	2.47	340
Decouple aggregation	DBStereo-S (Ours)	0.65	2.36	15
	DBStereo-M (Ours)	0.50	1.80	33
	DBStereo-L (Ours)	0.45	1.57	49

5.3 Benchmark datasets and Performance

We evaluate our DBStereo on two widely used benchmarks and submit the results to online leaderboards for public comparison: Scene Flow, KITTI 2012 and KITTI 2015.

Scene Flow: As shown in Table 1, we compare our proposed DBStereo and its variances with several state-of-the-art approaches on the SceneFlow dataset. Our DBStereo-L achieves the highest accuracy among all the published real-time methods and even surpass many high-performance iterative-based methods both accuracy and inference time such as RAFT-Stereo and IGEV-Stereo, reducing the runtime by more than 85%.

6 Conclusion

In this paper, we provide a thorough analysis of the limitations of traditional aggregation paradigm methods, breaking the empirical approach of using dimension-matched convolutions for a high-dimensional cost volume. We propose the DBStereo which is based on pure 2D convolutions but achieve impressive performance both in accuracy and inference time. DBStereo is a simple yet strong baseline of our proposed decouple aggregation paradigm. We hope our research will provide some insightful directions for future community studies.

References

- [1] A. Bangunharcana, J. W. Cho, S. Lee, I. S. Kweon, K.-S. Kim, and S. Kim. Correlate-and-excite: Real-time stereo matching via guided cost volume excitation. In *2021 IEEE/RSJ International Conference on Intelligent Robots and Systems (IROS)*, pages 3542–3548. IEEE, 2021.
- [2] J.-R. Chang and Y.-S. Chen. Pyramid stereo matching network. In *Proceedings of the IEEE Conference on Computer Vision and Pattern Recognition (CVPR)*, June 2018.
- [3] J. Cheng, W. Yin, K. Wang, X. Chen, S. Wang, and X. Yang. Adaptive fusion of single-view and multi-view depth for autonomous driving. In *Proceedings of the IEEE/CVF Conference on Computer Vision and Pattern Recognition*, pages 10138–10147, 2024.

- [4] J. Deng, W. Dong, R. Socher, L.-J. Li, K. Li, and L. Fei-Fei. Imagenet: A large-scale hierarchical image database. In *2009 IEEE Conference on Computer Vision and Pattern Recognition*, pages 248–255, 2009.
- [5] S. Duggal, S. Wang, W.-C. Ma, R. Hu, and R. Urtasun. Deeppruner: Learning efficient stereo matching via differentiable patchmatch. In *Proceedings of the IEEE/CVF international conference on computer vision*, pages 4384–4393, 2019.
- [6] S. Duggal, S. Wang, W.-C. Ma, R. Hu, and R. Urtasun. Deeppruner: Learning efficient stereo matching via differentiable patchmatch. In *Proceedings of the IEEE/CVF International Conference on Computer Vision*, pages 4384–4393, 2019.
- [7] S. Duggal, S. Wang, W.-C. Ma, R. Hu, and R. Urtasun. Deeppruner: Learning efficient stereo matching via differentiable patchmatch. In *Proceedings of the IEEE/CVF International Conference on Computer Vision (ICCV)*, October 2019.
- [8] A. Geiger, P. Lenz, and R. Urtasun. Are we ready for autonomous driving? the kitti vision benchmark suite. In *2012 IEEE Conference on Computer Vision and Pattern Recognition*, pages 3354–3361. IEEE, 2012.
- [9] X. Guo, K. Yang, W. Yang, X. Wang, and H. Li. Group-wise correlation stereo network. In *Proceedings of the IEEE/CVF Conference on Computer Vision and Pattern Recognition (CVPR)*, June 2019.
- [10] Y.-Z. Hsieh and S.-S. Lin. Robotic arm assistance system based on simple stereo matching and q-learning optimization. *IEEE Sensors Journal*, 20(18):10945–10954, 2020.
- [11] A. Kendall, H. Martirosyan, S. Dasgupta, P. Henry, R. Kennedy, A. Bachrach, and A. Bry. End-to-end learning of geometry and context for deep stereo regression. In *Proceedings of the IEEE International Conference on Computer Vision (ICCV)*, Oct 2017.
- [12] S. Khamis, S. Fanello, C. Rhemann, A. Kowdle, J. Valentin, and S. Izadi. Stereonet: Guided hierarchical refinement for real-time edge-aware depth prediction. In *Proceedings of the European conference on computer vision (ECCV)*, pages 573–590, 2018.
- [13] X. Li, C. Zhang, W. Su, and W. Tao. Iinet: Implicit intra-inter information fusion for real-time stereo matching. In *Proceedings of the AAAI Conference on Artificial Intelligence*, volume 38, pages 3225–3233, 2024.
- [14] Z. Liang, Y. Guo, Y. Feng, W. Chen, L. Qiao, L. Zhou, J. Zhang, and H. Liu. Stereo matching using multi-level cost volume and multi-scale feature constancy. *IEEE Transactions on Pattern Analysis and Machine Intelligence*, 43(1):300–315, 2019.
- [15] L. Lipson, Z. Teed, and J. Deng. Raft-stereo: Multilevel recurrent field transforms for stereo matching. In *2021 International Conference on 3D Vision (3DV)*, pages 218–227, 2021.
- [16] L. Lipson, Z. Teed, and J. Deng. Raft-stereo: Multilevel recurrent field transforms for stereo matching. In *2021 International Conference on 3D Vision (3DV)*, pages 218–227. IEEE, 2021.
- [17] N. Mayer, E. Ilg, P. Hausser, P. Fischer, D. Cremers, A. Dosovitskiy, and T. Brox. A large dataset to train convolutional networks for disparity, optical flow, and scene flow estimation. In *Proceedings of the IEEE Conference on Computer Vision and Pattern Recognition*, pages 4040–4048, 2016.
- [18] M. Menze and A. Geiger. Object scene flow for autonomous vehicles. In *Proceedings of the IEEE Conference on Computer Vision and Pattern Recognition*, pages 3061–3070, 2015.
- [19] G.-Y. Nie, M.-M. Cheng, Y. Liu, Z. Liang, D.-P. Fan, Y. Liu, and Y. Wang. Multi-level context ultra-aggregation for stereo matching. In *Proceedings of the IEEE/CVF Conference on Computer Vision and Pattern Recognition*, pages 3283–3291, 2019.
- [20] M. Sandler, A. Howard, M. Zhu, A. Zhmoginov, and L.-C. Chen. Mobilenetv2: Inverted residuals and linear bottlenecks. In *Proceedings of the IEEE Conference on Computer Vision and Pattern Recognition (CVPR)*, June 2018.
- [21] F. Shamsafar, S. Woerz, R. Rahim, and A. Zell. Mobilestereonet: Towards lightweight deep networks for stereo matching. In *Proceedings of the IEEE/CVF Winter Conference on Applications of Computer Vision (WACV)*, pages 2417–2426, January 2022.
- [22] V. Tankovich, C. Hane, Y. Zhang, A. Kowdle, S. Fanello, and S. Bouaziz. Hitnet: Hierarchical iterative tile refinement network for real-time stereo matching. In *Proceedings of the IEEE/CVF conference on computer vision and pattern recognition*, pages 14362–14372, 2021.

- [23] Q. Wang, S. Shi, S. Zheng, K. Zhao, and X. Chu. Fadnet++: Real-time and accurate disparity estimation with configurable networks. *arXiv preprint arXiv:2110.02582*, 2021.
- [24] X. Wang, G. Xu, H. Jia, and X. Yang. Selective-stereo: Adaptive frequency information selection for stereo matching. In *Proceedings of the IEEE/CVF Conference on Computer Vision and Pattern Recognition*, pages 19701–19710, 2024.
- [25] X. Wei, J. Liu, D. Yang, J. Cheng, C. Shu, and W. Wang. A wavelet-based stereo matching framework for solving frequency convergence inconsistency. *arXiv preprint arXiv:2505.18024*, 2025.
- [26] B. Wen, M. Trepte, J. Aribido, J. Kautz, O. Gallo, and S. Birchfield. Foundationstereo: Zero-shot stereo matching. In *Proceedings of the IEEE/CVF Conference on Computer Vision and Pattern Recognition (CVPR)*, pages 5249–5260, June 2025.
- [27] Z. Wu, X. Wu, X. Zhang, S. Wang, and L. Ju. Semantic stereo matching with pyramid cost volumes. In *Proceedings of the IEEE/CVF International Conference on Computer Vision*, pages 7484–7493, 2019.
- [28] G. Xu, J. Cheng, P. Guo, and X. Yang. Attention concatenation volume for accurate and efficient stereo matching. In *Proceedings of the IEEE/CVF Conference on Computer Vision and Pattern Recognition (CVPR)*, pages 12981–12990, June 2022.
- [29] G. Xu, J. Liu, X. Wang, J. Cheng, Y. Deng, J. Zang, Y. Chen, and X. Yang. Banet: Bilateral aggregation network for mobile stereo matching. *arXiv preprint arXiv:2503.03259*, 2025.
- [30] G. Xu, X. Wang, X. Ding, and X. Yang. Iterative geometry encoding volume for stereo matching. In *Proceedings of the IEEE/CVF Conference on Computer Vision and Pattern Recognition (CVPR)*, pages 21919–21928, June 2023.
- [31] G. Xu, X. Wang, X. Ding, and X. Yang. Iterative geometry encoding volume for stereo matching. In *Proceedings of the IEEE/CVF Conference on Computer Vision and Pattern Recognition*, pages 21919–21928, 2023.
- [32] G. Xu, Y. Wang, J. Cheng, J. Tang, and X. Yang. Accurate and efficient stereo matching via attention concatenation volume. *IEEE Transactions on Pattern Analysis and Machine Intelligence*, 46(4):2461–2474, 2023.
- [33] H. Xu and J. Zhang. Aanet: Adaptive aggregation network for efficient stereo matching. In *Proceedings of the IEEE/CVF conference on computer vision and pattern recognition*, pages 1959–1968, 2020.
- [34] H. Xu and J. Zhang. Aanet: Adaptive aggregation network for efficient stereo matching. In *Proceedings of the IEEE/CVF Conference on Computer Vision and Pattern Recognition (CVPR)*, June 2020.
- [35] G. Yang, X. Song, C. Huang, Z. Deng, J. Shi, and B. Zhou. Drivingstereo: A large-scale dataset for stereo matching in autonomous driving scenarios. In *Proceedings of the IEEE/CVF Conference on Computer Vision and Pattern Recognition*, pages 899–908, 2019.
- [36] N. Zenati and N. Zerhouni. Dense stereo matching with application to augmented reality. In *2007 IEEE International Conference on Signal Processing and Communications*, pages 1503–1506. IEEE, 2007.
- [37] D. Zheng, X.-M. Wu, Z. Liu, J. Meng, and W.-s. Zheng. Diffuvolume: Diffusion model for volume based stereo matching. *International Journal of Computer Vision*, 133(7):3807–3821, 2025.